

Black Hole Excision for Dynamic Black Holes

Miguel Alcubierre⁽¹⁾, Bernd Brügmann⁽¹⁾, Denis Pollney⁽¹⁾, Edward Seidel^(1,2), Ryoji Takahashi⁽¹⁾

⁽¹⁾ Max-Planck-Institut für Gravitationsphysik, Am Mühlenberg 1, D-14476 Golm, Germany

⁽²⁾ National Center for Supercomputing Applications, Beckman Institute, 405 N. Mathews Ave., Urbana, IL 61801

(April 26, 2024; AEI-2001-021)

We extend previous work on 3D black hole excision to the case of distorted black holes, with a variety of dynamic gauge conditions that are able to respond naturally to the spacetime dynamics. We show that the combination of excision and gauge conditions we use is able to drive highly distorted, rotating black holes to an almost static state at late times, with well behaved metric functions, without the need for any special initial conditions or analytically prescribed gauge functions. Further, we show for the first time that one can extract accurate waveforms from these simulations, with the full machinery of excision and dynamic gauge conditions. The evolutions can be carried out for long times, far exceeding the longevity and accuracy of even better resolved 2D codes. While traditional 2D codes show errors in quantities such as apparent horizon mass of over 100% by $t \approx 100M$, and crash by $t \approx 150M$, with our new techniques the same systems can be evolved for hundreds of M's in full 3D with errors of only a few percent.

04.25.Dm, 04.30.Db, 97.60.Lf, 95.30.Sf

Introduction. The long term numerical evolution of black hole (BH) systems is one of the most challenging and important problems in numerical relativity. For BHs, the difficulties of accuracy and stability in solving Einstein's equations numerically are exacerbated by the special problems posed by spacetimes containing singularities. At a singularity, geometric quantities become infinite and cannot be handled easily by a computer.

Traditionally, in the 3+1 approach the freedom in choosing the slicing is used to slow down the approach of the time slices towards the singularity ("singularity avoidance"), while allowing them to proceed outside the BH. Singularity avoiding slicings are able to provide accurate evolutions, allowing one to study BH collisions and extract waveforms [1], but only for limited cases and evolution times. Combining short full numerical evolutions with perturbation methods, one can even study the plunge from the last stable orbit of two BHs [2]. But a dramatic breakthrough is required to push numerical simulations far enough to study orbiting BHs, requiring accurate evolutions exceeding time scales of $t \approx 100M$. In 3D, traditional approaches have not been able to reach such time scales, even in the case of Schwarzschild BHs.

A more promising approach involves cutting away the singularity from the calculation ("singularity excision"), assuming it is hidden inside an apparent horizon (AH) [3,4]. Although this work has been progressing, from early spherical proof of principle in Ref. [4] to recent 3D developments [5–8], beyond a few spherical test cases [9,10] it has yet to be used in conjunction with appropriate live gauge conditions designed to respond to both the dynamics of the BH and the coordinate motion through the spacetime.

In this paper we extend recent excision work [7] to the case of distorted, dynamic BHs in 3D, using a new class of gauge conditions. These gauge conditions, which not

only respond naturally to the true spacetime dynamics, but also *drive the system towards an almost static state at late times*, allow us to handle BHs without considering special initial coordinate systems, such as the Kerr-Schild type, which may be difficult or impossible to find during a generic BH evolution. We show that not only are the evolutions accurate as indicated by the mass associated with the apparent horizon, but also that very accurate waveforms can be extracted with excision, even when the waves carry only a tiny fraction of the energy of the spacetime. Furthermore, we show that the 3D evolutions of dynamic BHs we are now able to perform, are superior, in terms of accuracy, stability, and longevity, to previous dynamic 3+1 BH simulations, whether they were carried out in full 3D or even when restricted to 2D. These results indicate that BH excision can be made to work under rather general circumstances, and can dramatically improve both the length of the evolutions, and the accuracy of the waveforms extracted, which will be crucial for gravitational wave astronomy.

Initial Data. For this paper we consider a series of single distorted BH spacetimes [11,12] that have been used to model the late stages of BH coalescence [13,14]. Following [11,12], the initial three-metric γ_{ab} is chosen to be

$$ds^2 = \Psi^4 [e^{2q} (d\eta^2 + d\theta^2) + \sin^2 \theta d\phi^2], \quad (1)$$

where the "Brill wave" function q is a general function of the spatial coordinates, subject to certain regularity and fall off restrictions, that can be tailored to produce very distorted 3D BHs interacting with nonlinear waves. The radial coordinate η is logarithmic in the cartesian radius r . There are two classes of data sets used here corresponding to even- and odd-parity distortions. The even-parity data have vanishing extrinsic curvature, while the cases containing an odd-parity component have nontriv-

ial extrinsic curvature K_{ij} . As shown in [15,16], these distorted BH data sets can include rotation as well, corresponding to spinning, distorted BHs that mimic the early merger of two orbiting BHs. Hence they make an ideal test case for the development of our techniques. We leave the details of the construction of these BH initial data sets to Refs. [15,16].

An important point that we wish to emphasize is that such data are *not* of the Kerr-Schild form with ingoing coordinates at the horizon. That particular form of BH initial data sets has been recently advocated as providing a more natural treatment for BH excision since the coordinate system is adapted to inward propagation of quantities at the horizon [17]. However, it is not obvious that the physically desired initial data can always be written in the Kerr-Schild form (or, for that matter, in any other particular form). Furthermore, during an evolution, even if similar such coordinates are somehow actively enforced, it is probably not possible to have such a coordinate system in place at all times, when a new BH forms. Hence, we prefer to be able to handle BH data in any coordinate system, and apply coordinate conditions that naturally drive the system into a static state as the BH system settles down to Kerr, from any starting point.

Evolution and Excision Procedures. Our simulations have been performed using what we refer to as the “BSSN” version of the 3+1 evolution equations [18–21], which we have found to have superior stability properties when compared to standard formulations. As detailed in [20–22], in this paper we also actively force the trace of the conformal-traceless extrinsic curvature \tilde{A}_{ij} to remain zero, and we use the independently evolved “conformal connection functions” $\tilde{\Gamma}^i$ only in terms where derivatives of these functions appear.

We use the simple excision approach described in [7]. Our excision algorithm is based on the following ideas: (a) Excise a *cube* contained inside the AH that is well adapted to cartesian coordinates; (b) Use a simple but stable boundary condition at the sides of the excised cube: copying of time derivatives from their values one grid point out along the normal directions; (c) Use standard centered (non-causal) differences in all terms except for advection terms on the shift (those that look like $\beta^i \partial_i$). For these terms we use second order upwind along the shift direction. These simplifications in excision reduce the complexity in the algorithm, avoid delicate interpolation issues near the excision boundary, and have allowed us to make rapid progress.

Gauge Conditions. We have used both elliptic and hyperbolic slicing conditions, but we focus here on the hyperbolic conditions. Consider the “K freezing” condition (e.g. [7]), $\partial_t K = 0$, where K is the trace of the extrinsic curvature. This is an elliptic equation for the lapse, which in the particular case $K = 0$ reduces to the maximal slicing condition. Here we propose the following evolution equation for the lapse,

$$\partial_t^2 \alpha = -\alpha^2 f(\alpha) \partial_t K, \quad (2)$$

for which the lapse will evolve as long as both $\alpha f(\alpha)$ and $\partial_t K$ are non-vanishing. Here f is a (positive) function of α which we specify below, motivated by the Bona-Massó family of slicing conditions [23]. A key feature of this new lapse condition is that even in the presence of a shift vector and when K is non-zero, the system can reach a state for which $\partial_t K = 0$ for the final, stationary black hole.

For the shift β^i we have experimented with families of elliptic, parabolic, and hyperbolic conditions that relate the shift choice with the evolution of the BSSN conformal connection functions $\tilde{\Gamma}^i$. We obtain parabolic and hyperbolic shift prescriptions by making either $\partial_t \beta^i$ or $\partial_t^2 \beta^i$ proportional to the elliptic operator for β^i contained in the condition $\partial_t \tilde{\Gamma}^k = 0$, which we call “Gamma freezing” in Ref. [22], and which is closely related to the well known minimal distortion family of gauge conditions [24]. The hyperbolic condition has the form

$$\partial_t^2 \beta^i = \frac{k}{\Psi^4} \partial_t \tilde{\Gamma}^i - \eta \partial_t \beta^i, \quad (3)$$

where both k and η are positive constants, and Ψ is the time independent conformal factor of the initial data defined in (1). We call such evolution conditions for the lapse and the shift hyperbolic “driver” conditions (see [25]).

In the spirit of the puncture method for evolutions [26], we use a BSSN scheme with the usual time-dependent conformal factor $e^{4\phi}$ and an additional time-independent conformal factor Ψ^4 . The division by Ψ^4 in (3) helps to slow down the evolution of the shift in the vicinity of the black hole. We have also found it important to add a dissipation term with coefficient η in order to reduce some initial transient oscillations in the shift. Notice that in contrast with k , the coefficient η is not dimensionless (it has dimensions of inverse length), so in practice we rescale it using the total mass of the system. Experience has shown that by tuning the value of the dissipation coefficient we can almost freeze the evolution of the system at late times.

The parameters used for all simulations described below are: α is given by Eq. (2), with $f = 2/\alpha$; β^i is given by Eq. (3) with $k = 0.75$, $\eta = 3/M$ (where M is the initial ADM mass of the system). As initial data we take ($\alpha = 1$, $\beta^i = 0$, $\partial_t \alpha = \partial_t \beta^i = 0$) except in one case mentioned below where we perform a single maximal slicing solve to obtain a more appropriate initial lapse. Given this initial data for lapse and shift, we let the evolution equations take care of the rest. We stress that we have not used any special information about the coordinates or type of the initial data used. Further, we use the same gauge parameters for all results in this paper, whether they are applied to Schwarzschild, distorted, or rotating BHs, showing the strength and generic nature of these conditions.

Results. The first example we show is Schwarzschild, written in the standard isotropic coordinates used in many BH evolutions. Note that with this initial data

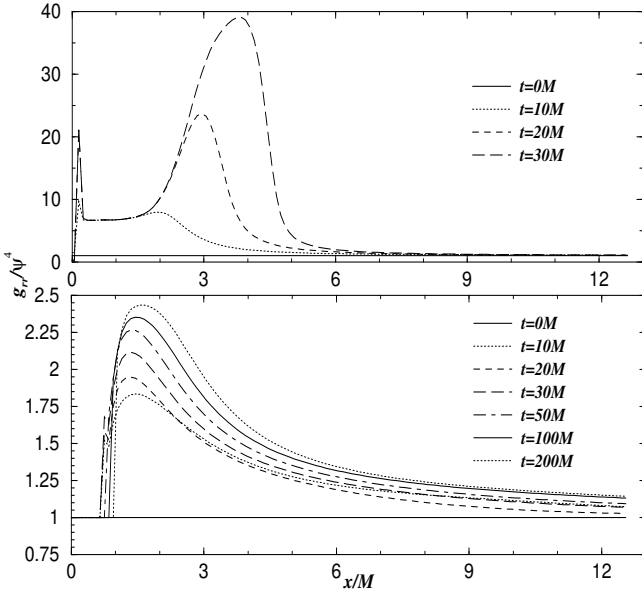


FIG. 1. We show the radial metric function g_{rr}/Ψ^4 for a Schwarzschild BH along the x -axis, constructed from the cartesian metric components, as it evolves with time. The upper panel shows the grid-stretching in the metric for singularity avoiding slicing with vanishing shift and no excision, while the lower panel shows the metric for the new gauge conditions with an excision box inside a sphere of radius $1M$. Note the difference in the vertical scales. Without shift and excision the metric grows out of control, while with shift and excision a peak begins to form initially as grid stretching starts, but later freezes in as the shift drives the BH into a static configuration (note the time labels).

and our starting gauge conditions, the BH should evolve rapidly. If α and β^i were held fixed at their initial values, the slice would hit the singularity at $t = \pi M$ and crash. Instead, α and β^i work together with the excision to rapidly drive the system towards a static state, without any special choice of initial conditions.

In Fig. 1 we show the radial metric function g_{rr}/Ψ^4 vs. time. The grid covers an octant with 128^3 points ($\Delta x = 0.1M$, $M = 2$). Notice that the metric begins to grow, as it does without a shift, but as the shift builds up the growth slows down significantly. At this stage, the system is effectively static, even though we started in the highly dynamic isotropic coordinates. We also show the time development of α and β^i in Fig. 2, which evolve rapidly at first but then effectively freeze, bringing the system towards an almost static configuration by $t = 10M$. The evolution then proceeds only very slowly until the simulation is stopped well after $t = 200M$.

In Fig. 3 we show the AH mass M_{AH} , determined with a 3D AH finder [27]. For comparison, we also show the value of M_{AH} obtained from a highly resolved 2D simulation with zero shift and no excision, and for the 3D run without shift. While the 3D simulation with shift and excision continues well beyond $t = 200M$, the 2D re-

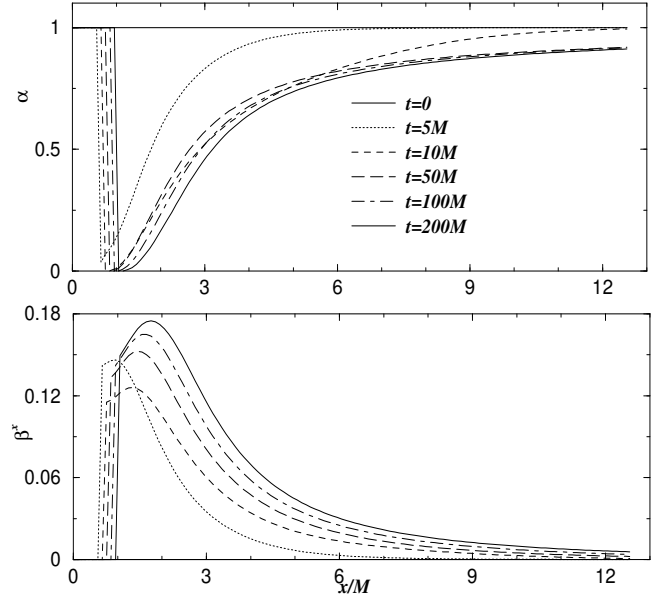


FIG. 2. We show the lapse and shift for the excision evolution of a Schwarzschild BH. After around $10M$, the lapse and shift freeze in as the system is driven to a static configuration. The size of the excision box was allowed to grow with the change in the coordinate location of the AH.

sult becomes very inaccurate and the code crashes due to axis instabilities by $t = 150M$, and the 3D run without shift crashes already by $t = 50M$. Notice that in the 2D case, after around $t = 35M$, M_{AH} grows rapidly due to numerical errors associated with grid stretching, and the AH finder ultimately fails as the code crashes. With excision and our new gauge conditions, the 3D run has less than a few percent error by $t = 200M$, while the 2D case has more than 100% error before it crashes at $t \approx 150M$. For the excision run, notice also that while there is some initial evolution in the metric and the coordinate size of the AH (see Figs. 1 and 2) the AH mass changes only very little.

Next, we turn to a truly dynamic, even-parity distorted BH. This system contains a strong gravitational wave that distorts the BH, causing it to evolve, first nonlinearly, and then oscillating at its quasi-normal frequency, finally settling down to a static Schwarzschild BH. This provides a test case for our techniques with dynamic, evolving BH spacetimes, and allows us to test our ability to extract gravitational waves with excision for the first time. In this case, in the language of [15], we choose the Brill wave parameters to be $Q_0 = 0.5$, $\eta_0 = 0$, $\sigma = 1$, corresponding to a highly distorted BH with $M = 1.83$.

In Fig. 4 we show the AH mass M_{AH} as a function of time for the distorted BH simulations carried out in both 2D and 3D. M_{AH} grows initially as a nonlinear burst of gravitational waves is absorbed by the BH, distorting it strongly, but then levels off as the BH goes into a ring-down phase towards Schwarzschild. Fig. 5 shows the polar circumference of the apparent horizon divided

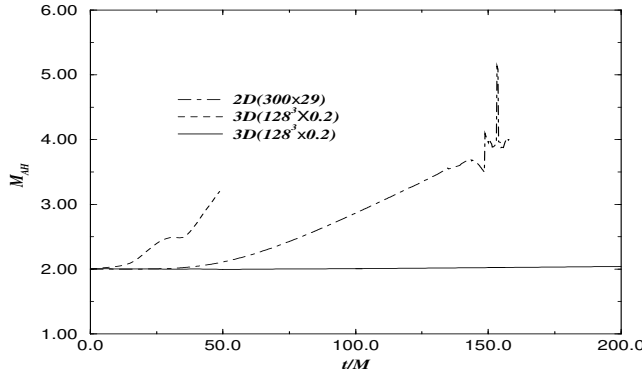


FIG. 3. The solid line shows the development of the AH mass M_{AH} , determined through a 3D AH finder, for the excision simulation of a Schwarzschild BH shown above, while the dashed lines show the AH mass obtained using 2D and 3D codes with zero shift and no excision. The 2D code crashes at around $t = 150M$, the 3D run without shift crashes around $t = 50M$, while the 3D run with shift and excision reaches an effectively static state and the error remains less than a few percent even after $t = 200M$.

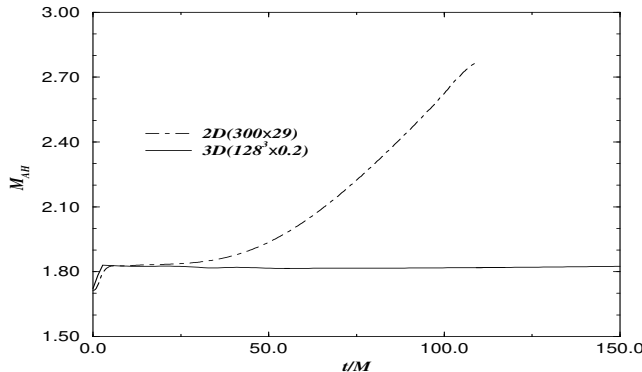


FIG. 4. We show the AH masses M_{AH} for a BH with even-parity distortion for the 2D (no excision, no shift) and 3D (excision, shift) cases. The 3D result continues well past $150M$, while the 2D result becomes very inaccurate and crashes by $t = 100M$.

by the equatorial circumference. This ratio allows an estimate of the size of the local dynamics during the run. Notice how the horizon starts far from spherical (with an initial ratio close to 2), it later oscillates from prolate to oblate and back again, and finally settles on a sphere (with a ratio of 1).

In the 3D case, the dynamic gauge conditions and excision quickly drive the evolution towards an almost static configuration, as the system itself evolves towards a static Schwarzschild BH. The evolution is continued until terminated at around $t = 160M$. Even in this highly dynamic system, no specialized form of initial data or lapse and shift are needed; our gauge choices naturally drive the system to a static state as desired. To our knowledge, distorted BHs of this type have never been evolved for so long, nor with such accuracy, in either 2D or 3D. By comparison, in the more highly resolved 2D case with

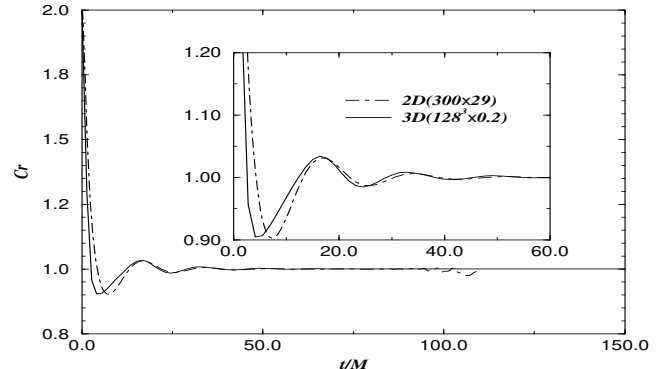


FIG. 5. As a measure for the dynamics of the apparent horizon for the BH with even-parity distortion we show the ratio of the polar and equatorial circumferences.

zero shift and no excision, the familiar grid stretching effects allowed by the gauge choice lead to highly inaccurate evolutions after some time with the error in M_{AH} again approaching 100% when the code finally crashes at $t \approx 100M$.

In Fig. 6, we show the results of extracting waves from the evolution of this highly distorted, excised BH. Using the standard gauge-invariant waveform extraction technique, the Zerilli function is shown for both the 2D and 3D simulations discussed above. There is a slight but physically irrelevant phase difference in the two results due to differences in the slicing; otherwise the results are remarkably similar. This shows conclusively that the excision and live gauge conditions do not adversely affect the waveforms, even if they carry a small amount of energy (around $10^{-3}M_{ADM}$ in this case).

We now turn to a rather different type of distorted BH, including rotation and general even- and odd-parity distortions. In the language of Ref. [15], the parameters for this simulation are $Q_0 = 0.5$, $\eta_0 = 0$, $\sigma = 1$, $J = 35$, corresponding to a rotating distorted BH with $M = 7.54$ and an effective rotation parameter $a/M = 0.62$. Previously, such data sets could be evolved only to about $40M$ [14]. Again, for the purposes of this paper we have chosen an axisymmetric case so that we can compare the results to those obtained with a 2D code. Since this example is much more demanding, we have found it important in order to increase the accuracy of our runs to perform a single initial maximal solve to reduce the initial gauge dynamics. The gauge conditions used work well even in the presence of rotation: the shift drives the system towards a static Kerr BH spacetime after the true dynamics settle down. The metric functions (not shown) evolve in a similar way to those shown before, essentially freezing at late times. In Fig. 7, we show the extracted waveforms, now computed using the imaginary part of the Newman-Penrose quantity Ψ_4 (e.g. [2]), which includes contributions from all ℓ -modes at the same time. The results from the 2D and 3D codes agree very closely, except for a slight phase shift due to slicing differences, until the 2D code becomes inaccurate and later crashes.

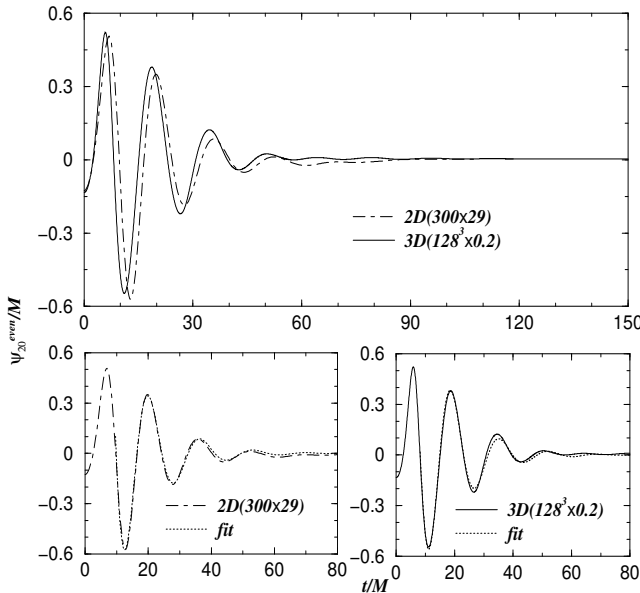


FIG. 6. The solid line shows the result of the $\ell = 2, m = 0$ waveform extraction at a radius $5.45M$ for the even-parity distorted BH described on the text, while the dashed line shows the result of the same simulation carried out in the 2D code. We also show a fit to the two lowest QNM's of the BH for 2D and 3D separately, using numerical data from $t = 9M$ to $t = 80M$.

The 3D simulation continues well beyond this point, and is terminated at $t = 120M$.

Conclusions. We have extended recently developed 3D BH excision techniques, using a new class of live gauge conditions that *dynamically drive* the BH system towards an essentially static state at late times, when the system itself settles to a stationary Kerr BH. Our techniques have been tested on highly distorted, rotating BHs, are shown to be very robust, and require no special coordinate systems or special forms of initial data. For the first time, excision is tested with wave extraction, and waveforms are presented and verified. The results are shown to be more accurate, and much longer lived, than previous 3D simulations and even better resolved 2D simulations of the same initial data. Such improvements in BH excision are badly needed for more astrophysically realistic BH collision simulations, which are in progress and will be reported elsewhere.

Acknowledgements. This work was supported by AEI. Calculations were performed using the Cactus code at AEI, NCSA, PSC, and RZG.

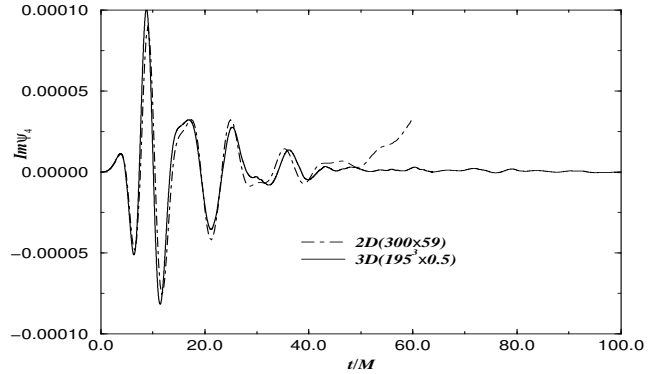


FIG. 7. The solid line shows the a imaginary part of ψ_4 at a radius $3.94M$ and $\theta = \phi = \pi/4$ for rotating 3D distorted BH, while the dash line shows the same initial date by the 2D code which crashes around $60M$.

(1987).

- [4] E. Seidel and W.-M. Suen, Phys. Rev. Lett. **69**, 1845 (1992).
- [5] G. B. Cook *et al.*, Phys. Rev. Lett **80**, 2512 (1998).
- [6] R. Gomez *et al.*, Phys. Rev. Lett. **80**, 3915 (1998), gr-qc/9801069.
- [7] M. Alcubierre and B. Brügmann, (2000), gr-qc/0008067.
- [8] S. Brandt *et al.*, , submitted, gr-qc/0009047.
- [9] P. Anninos *et al.*, Phys. Rev. D **52**, 2059 (1995).
- [10] G. E. Dauv, Ph.D. thesis, Washington University, St. Louis, Missouri, 1996.
- [11] S. Brandt and E. Seidel, Phys. Rev. D **54**, 1403 (1996).
- [12] S. Brandt and E. Seidel, Phys. Rev. D **52**, 856 (1995).
- [13] K. Camarda and E. Seidel, Phys. Rev. D **59**, 064026 (1999), gr-qc/9805099.
- [14] J. Baker *et al.*, Phys. Rev. D **62**, 127701 (2000), gr-qc/9911017.
- [15] S. Brandt, K. Camarda, and E. Seidel, in *Proceedings of the 8th Marcel Grossmann Meeting on General Relativity*, edited by T. Piran (World Scientific, Singapore, 1999), pp. 741–743.
- [16] S. Brandt, K. Camarda, and E. Seidel, in preparation (unpublished).
- [17] R. A. Matzner, M. F. Huq, and D. Shoemaker, Phys. Rev. D **59**, 024015 (1999).
- [18] M. Shibata and T. Nakamura, Phys. Rev. D **52**, 5428 (1995).
- [19] T. W. Baumgarte and S. L. Shapiro, Physical Review D **59**, 024007 (1999).
- [20] M. Alcubierre *et al.*, Phys. Rev. D **61**, 041501 (2000), gr-qc/9904013.
- [21] M. Alcubierre *et al.*, Phys. Rev. D **62**, 124011 (2000), gr-qc/9908079.
- [22] M. Alcubierre *et al.*, Phys. Rev. D **62**, 044034 (2000), gr-qc/0003071.
- [23] C. Bona, J. Massó, E. Seidel, and J. Stela, Phys. Rev. Lett. **75**, 600 (1995).
- [24] L. Smarr and J. York, Phys. Rev. D **17**, 2529 (1978).
- [25] J. Balakrishna *et al.*, Class. Quant. Grav. **13**, L135 (1996).
- [26] B. Brügmann, Int. J. Mod. Phys. D **8**, 85 (1999).
- [27] M. Alcubierre *et al.*, Class. Quant. Grav. **17**, 2159 (2000).

- [1] M. Alcubierre *et al.*, (2000), gr-qc/0012079.
- [2] J. Baker *et al.*, (2001), gr-qc/0102037.
- [3] J. Thornburg, Classical and Quantum Gravity **4**, 1119